DALTON
FULL PAPER

Neutral and cationic biimidazoledihalogenobis(trimethylphosphine)-rhenium(III) complexes: ion-pairing, acid–base and redox properties †

Sébastien Fortin,[a] Paul-Louis Fabre,[b] Michèle Dartiguenave[b] and André L. Beauchamp*[a]

[a] *Département de Chimie, Université de Montréal, C. P. 6128, Succ. Centre-Ville, Montréal (QC), H3C3J7, Canada. E-mail: beauchmp@chimie.umontreal.ca*
[b] *Laboratoire de Chimie Inorganique, Université Paul Sabatier, 118 route de Narbonne, 31062 Toulouse, France*

Received 23rd April 2001, Accepted 4th September 2001
First published as an Advance Article on the web 15th November 2001

Cationic Re(III) complexes $[ReX_2(PMe_3)_2(biimH_2)]X$ (where $biimH_2$ = 2,2′-biimidazole; X = Cl, Br, I) are prepared by phosphine displacement in the corresponding PPh_3 complexes in the presence of excess PMe_3. The N–H protons of co-ordinated biimidazole are moderately acidic and the monodeprotonated form $[ReX_2(PMe_3)_2(biimH)]$ is isolated after addition of one equivalent of $NaOCH_3$. Crystal structures determined for two compounds of each series reveal that strong hydrogen bonding takes place between the N–H groups and the halide counter-ion in the cationic complexes, whereas the neutral molecules crystallise as dimeric units tightly associated *via* two complementary N–H ··· N interactions. The acidities of the two N–H groups of $[ReCl_2(PMe_3)_2(biimH_2)]^+$ in CH_2Cl_2 are estimated from UV-visible spectra and found to correspond approximately to those of formic acid and 3-chlorophenol, respectively. Electrochemical data on the series of PPh_3 and PMe_3 complexes with the three halides indicate that the redox potentials of both the metal and the counter-ion are affected by ion pairing in solution.

Introduction

Our research group has developed an interest in the complexation of rhenium to 2,2′-biimidazole ($biimH_2$) and its derivatives for various reasons. Firstly, being a chelating agent, it can stabilise co-ordination arrangements that have been found, with monodentate imidazoles,[1–3] to lead to spectral properties substantially different from those of similar systems with pyridines or related ligands.[4–7] Secondly, the residual N–H groups on co-ordinated biimidazole can be used to design supramolecular materials assembled *via* controlled hydrogen-bonding interactions.[8–10] Thirdly, since its anion is a potentially bis-bidentate bridging unit, it may be used as a link to connect metal centres into larger building blocks[11–13] and develop molecular devices.[14,15] Electron transfer is believed to be favoured in such systems with a short metal–metal distance and a rigid conjugated bridging ligand.[15] It has been stated that biimidazole promotes the communication between metal centres *via* orbital interactions,[16,17] which leads to high sensitivity of the redox and spectral features[18] of interest for switch systems.

In our previous contribution,[19] we reported that Re(V) precursors $ReOX_3(PPh_3)_2$ or $ReO(OEt)X_2(PPh_3)_2$ can be reduced cleanly in the presence of biimidazole, giving good yields of the rhenium(III) cationic complexes *cis*,*trans*-$[ReX_2(PPh_3)_2(biimH_2)]X$ with X = Cl, Br and I. The residual N–H protons of co-ordinated $biimH_2$ were found to be moderately acidic and to participate in strong hydrogen-bonding interactions, leading to tight ion pairs with halide or carboxylate counter-ions. These are interesting features for a starting block to be assembled into supramolecular architectures or polymetallic units. However, the presence of the bulky PPh_3 ligands precludes the formation of larger species. Therefore, attempts were made to replace PPh_3 by a smaller phosphine. We wish to describe here the preparation and structure of the compounds obtained by substitution of PPh_3 with PMe_3, together with their acid–base and redox properties.

Experimental

Reactants and methods

Tetrabutylammonium hexafluorophosphate (Fluka), iodide (Merck), bromide (Acros) and chloride (Aldrich), trimethylphosphine (PMe_3 97%, Aldrich), sodium methoxide (25% solution in methanol, Aldrich), solvents and other chemicals were used as received. Compounds $[ReCl_2(PPh_3)_2(biimH_2)]Cl$ (**1**), $[ReBr_2(PPh_3)_2(biimH_2)]Br$ (**2**) and $[ReI_2(PPh_3)_2(biimH_2)]I$ (**3**) were synthesised as reported previously.[19]

^1H NMR spectra were recorded at 300 MHz on a Bruker AMX-300 spectrometer or at 400 MHz on a Bruker ARX-400 instrument. The residual solvent signal was used as an internal standard ($CDCl_3$ 7.26 ppm) and the chemical shifts are reported with respect to Me_4Si. IR spectra were recorded as KBr pellets on a Perkin-Elmer 1750 FTIR spectrometer. UV-visible spectra were obtained as CH_2Cl_2 solutions on a Varian Cary 100 Bio spectrometer, using short path length cylindrical cells (type 136, 0.9 mm) from Quaracell. Elemental analyses were performed at the Laboratoire d'Analyse Élémentaire de l'Université de Montréal. Mass spectra were recorded as nitrobenzylic alcohol solutions at the Centre Régional de Spectrométrie de Masse de l'Université de Montréal. Magnetic moments were determined at the Laboratoire de Chimie de Coordination du CNRS, Toulouse, France. The measurements were made on solid samples at 25 °C by the Faraday method, using a Cahn microbalance coupled with a Drusch electromagnet. $HgCo(NCS)_4$ was used as standard ($\chi_g = 16.44 \times 10^{-6}$

† Electronic supplementary information (ESI) available: details of the structure determination and refinement for compounds **4**, **5**, **7** and **9**·$OPPh_3$. See http://www.rsc.org/suppdata/dt/b1/b103719f/

 DOI: 10.1039/b103719f

cgs emu) and corrections were applied for the diamagnetism of the ligands.[20]

Preparative work

[$ReCl_2(PMe_3)_2(biimH_2)$]Cl (4). To an orange suspension of **1** (205 mg; 0.215 mmol) in 50 mL of boiling benzene, 5 equivalents of PMe_3 were added dropwise. No obvious change occurred at first, but a clear orange solution was obtained after ≈30 minutes. After 6 hours, the solvent was evaporated to dryness *in vacuo*. The solid was filtered off and washed with diethyl ether. Yield: 100 mg, 80%. Recrystallisation in CH_2Cl_2/pentane afforded a pure compound. ^{1}H NMR ($CDCl_3$): δ 7.64 (s, 18H, 2 PMe_3), 0.74 (s, 2H, 2 H5), −2.15 (s, 2H, 2 H4). UV-visible (λ/nm ($\varepsilon \times 10^{-3}$/$M^{-1}$ cm^{-1})): 422 (3.28), 357 (2.59), 343 (2.03). Anal. Calc. for $C_{12}H_{24}Cl_3N_4P_2Re$: C, 24.90; N, 9.68; H, 4.18. Found: C, 25.13; N, 9.65; H, 4.48%. MS (FAB^+): *m*/*z* 541 $(M)^+$, 540 $(M - H)^+$, 465 $(M - PMe_3)^+$, 464 $(M - PMe_3 - H)^+$. $\mu_{eff} = 1.91\ \mu_B$. Crystals suitable for X-ray diffraction work were obtained by diffusion of diethyl ether vapour into a CH_2Cl_2 solution.

[$ReBr_2(PMe_3)_2(biimH_2)$]Br (5). The same method was used, starting with **2** (478 mg; 0.441 mmol). Yield: 100 mg, 60%. ^{1}H NMR ($CDCl_3$): δ 7.08 (s, 18H, 2 PMe_3), 1.25 (s, 2H, 2 H5), −2.09 (s, 2H, 2 H4). UV-visible (λ/nm ($\varepsilon \times 10^{-3}$/$M^{-1}$ cm^{-1})): 441 (4.09), 430 (4.40), 359 (4.46), 339 (4.86). Anal. Calc. for $C_{12}H_{24}Br_3N_4P_2Re$: C, 20.24; N, 7.87; H, 3.40. Found: C, 20.61; N, 7.81; H, 3.61%. MS (FAB^+): *m*/*z* 629 $(M)^+$, 628 $(M - H)^+$, 553 $(M - PMe_3)^+$, 552 $(M - PMe_3 - H)^+$. $\mu_{eff} = 1.76\ \mu_B$. Crystals suitable for X-ray diffraction were obtained by diffusion of diethyl ether vapour into a CH_2Cl_2 solution.

[$ReI_2(PMe_3)_2(biimH_2)$]I (6). Same procedure as above starting with **3** (506 mg; 0.41 mmol), but the reaction was carried out under argon. At the end of the reaction, the solvent was evaporated *in vacuo*. The sticky brown solid was dissolved in a minimum of CH_2Cl_2 and precipitated with hexanes. The brown solid was filtered off and washed with pentane. Yield: 261 mg, 73%. ^{1}H NMR ($CDCl_3$): δ 5.93 (s, 18H, 2 PMe_3), 2.33 (s, 2H, 2 H5), −2.38 (s, 2 H, 2 H4). UV-visible (λ/nm ($\varepsilon \times 10^{-3}$/$M^{-1}$ cm^{-1})): 493 (4.26), 443 (7.24), 385 (5.15), 336 (3.10). Anal. Calc. for $C_{12}H_{24}I_3N_4P_2Re$: C, 16.89; N, 6.57; H, 2.84. Found: C, 16.96; N, 6.36; H, 2.84%. MS (TOF LD^+): *m*/*z* 725 $(M)^+$, 724 $(M - H)^+$, 649 $(M - PMe_3)^+$, 648 $(M - PMe_3 - H)^+$. $\mu_{eff} = 1.72\ \mu_B$.

[$ReCl_2(PMe_3)_2(biimH)$] (7). To an orange solution of **4** (32 mg; 0.056 mmol) in 2 mL of methanol was added 1 equivalent of $NaOCH_3$. The colour turned red instantly and a solid appeared quickly. This red solid was filtered off and washed with methanol and diethyl ether. Yield: 15 mg, 50%. ^{1}H NMR ($CDCl_3$): δ 6.96 (s, 18H, 2 PMe_3), −4.23 (s, 2H, 2 H5), −6.96 (s, 2H, 2 H4). UV-visible (λ/nm ($\varepsilon \times 10^{-3}$/$M^{-1}$ cm^{-1})): 504 (0.271), 409 (3.25). Anal. Calc. for $C_{12}H_{23}Cl_2N_4P_2Re$: C, 26.57; N, 10.33; H, 4.27. Found: C, 26.66; N, 10.33; H, 4.43%. Crystals suitable for X-ray diffraction were obtained by diffusion of diethyl ether vapour into a CH_2Cl_2 solution.

[$ReBr_2(PMe_3)_2(biimH)$] (8). The above procedure to prepare **7** was applied to **5** (40 mg; 0.056 mmol) and a red solid was obtained (20 mg, 66%). Recrystallisation in CH_2Cl_2/Et_2O afforded a pure compound. ^{1}H NMR ($CDCl_3$): δ 6.25 (s, 18H, 2 PMe_3), −4.00 (s, 2H, 2 H5), −6.85 (s, 2H, 2 H4). Anal. Calc. for $C_{12}H_{23}Br_2N_4P_2Re$: C, 22.83; N, 8.87; H, 3.67. Found: C, 22.99; N, 8.74; H, 3.66%.

[$ReI_2(PMe_3)_2(biimH)$] (9). To an orange-brown solution of **6** (49 mg; 0.057 mmol) in 2 mL of methanol was added 1 equivalent of $NaOCH_3$. The colour turned dark brown and a solid appeared instantly. The dark red-brown solid was filtered off and washed with methanol and diethyl ether. Yield: 30 mg, 71%. The powder was recrystallised in CH_2Cl_2/Et_2O. ^{1}H NMR ($CDCl_3$): δ 4.71 (s, 18H, 2 PMe_3), −3.13 (s, very broad, 2 H5), −6.74 (s, very broad, 2 H4). Anal. Calc. for $C_{12}H_{23}I_2N_4P_2Re$: C, 19.87; N, 7.72; H, 3.20. Found: C, 20.14; N, 7.60; H, 3.10%.

Crystals of **9** containing "lattice" triphenylphosphine oxide were obtained when a diethyl ether solution of the crude reaction product was left in air overnight. The oxide is produced by oxidation of the PPh_3 ligand displaced by PMe_3, still present in the crude mixture.

Crystallographic measurements and structure determination

The crystals were glued on a glass fibre and mounted on a diffractometer. The X-ray work on **4**, **5** and **7** was done on an Enraf-Nonius CAD-4 instrument using CuKα radiation. The reduced triclinic cell was obtained from a preliminary search from an axial photograph.[21] For **9**, the study was conducted on a Siemens P4 diffractometer using MoKα radiation. An automatic search in the reciprocal sphere yielded the reduced cell.[22] In all cases, the unit cell was redefined when a more symmetric cell was indicated by the Niggli parameters, and Laue symmetry was determined from a fast data precollection, which also revealed the systematic absences. Laue symmetry and systematic absences were eventually checked from the full data set.

The data were corrected for absorption (NRCVAX package,[23] Gaussian integration based on crystal faces) and averaged.[24] The structures of **4**, **5** and **7** were solved by direct methods or Patterson syntheses of SHELXS-86[25] and ΔF syntheses of NRCVAX[23] and SHELXL-93.[26] The structure of **9** was solved by the Patterson method and ΔF syntheses of the Siemens SHELXTL package.[27] Non-hydrogen atoms were generally refined anisotropically. Hydrogen atoms were placed at idealised positions and refined as riding atoms with C–H distances of 0.93 (sp^2 C) or 0.96 Å (methyl), and N–H distances of 0.86 Å. Their isotropic displacement factors U_{iso} were adjusted 20% (sp^2 C and N) or 50% (methyl) above the value for the bonded atom. The VOID routine of the PLATON software[28] was used to check for the presence of holes in the structure. Crystal data of the four compounds are collected in Table 1. Details on structure determination and refinement for each compound are provided as Supplementary Information.†

CCDC reference numbers 171624–171627.

See http://www.rsc.org/suppdata/dt/b1/b103719f/ for crystallographic data in CIF or other electronic format.

Electrochemical measurements

All experiments were carried in freshly distilled and degassed CH_2Cl_2 containing 0.1 M NBu_4PF_6 as supporting electrolyte. A conventional cell was used for all types of experiments (CV, steady state voltammetry and linear sweep RDV), with SCE as reference electrode, a Pt wire as counter-electrode and a Pt disk as working electrode. The diameters of the working electrode were 0.5 mm, 0.0064 mm (calibrated with the ferrocene redox couple Fc/Fc^+) and 2 mm for CV, steady-state and RDV, respectively. The $E_{1/2}$ value for the Fc/Fc^+ couple is 420 mV with this system. Potential was controlled by an Autolab PGStat-20 potentiostat and the data were collected and analysed with the GPES software.[29] The cyclic voltammetry data listed in Table 3 were obtained at a sweep rate of 100 mV s^{-1}.

Results and discussion

Preparation and characterisation

The cationic [$ReX_2(PMe_3)_2(biimH_2)$]X compounds **4**–**6** form smoothly when the corresponding PPh_3 complexes are refluxed with excess of PMe_3 in benzene. Examples of phosphine substitution on rhenium compounds have been

Table 1 Crystallographic data

Compound	**4**·0.8$C_4H_{10}O$·0.4CH_2Cl_2	**5**·1.1$C_4H_{10}O$	**7**	**9**·$OPPh_3$
Empirical formula	$C_{12}H_{24}Cl_3N_4P_2Re$·0.8$C_4H_{10}O$·0.4CH_2Cl_2	$C_{12}H_{24}Br_3N_4P_2Re$·1.1$C_4H_{10}O$	$C_{12}H_{23}Cl_2N_4P_2Re$	$C_{12}H_{23}I_2N_4P_2Re$·$C_{18}H_{15}OP$
Formula weight	672.14	793.75	542.40	1003.55
a/Å	20.566(7)	12.952(10)	12.048(5)	9.488(2)
b/Å	20.566(7)	15.892(9)	9.150(3)	12.841(2)
c/Å	12.563(7)	15.898(10)	18.308(5)	30.166(4)
α/°	90	82.36(5)	90	90
β/°	90	69.27(6)	91.54(3)	101.660(10)
γ/°	90	68.09(6)	90	90
V/Å^3	5314(3)	2839(3)	2017.5(12)	3599.4(11)
Z	8	4	4	4
Space group	*I*4/*m* (no. 87)	$P\bar{1}$ (no. 2)	$P2_1/c$ (no. 14)	$P2_1/c$ (no. 14)
T/°C	20(2)	20(2)	20(2)	20(2)
λ/Å	1.54178 (CuKα)	1.54178 (CuKα)	1.54178 (CuKα)	0.71073 (MoKα)
ρ_{calcd}/g cm^{-3}	1.680	1.857	1.786	1.852
Crystal size/mm	0.48 × 0.17 × 0.14	0.53 × 0.14 × 0.14	0.70 × 0.36 × 0.06	0.40 × 0.20 × 0.16
μ/mm^{-1}	13.52	14.28	15.39	5.253
R^a ($I > 2\sigma(I)$)	0.0413	0.0388	0.0581	0.0409
$wR2^b$ ($I > 2\sigma(I)$)	0.1204	0.1042	0.1444	0.0809
S^c	1.118	1.139	1.042	1.100

^{a} $R1 = \Sigma(||F_o| - |F_c||)/\Sigma(|F_o|)$. ^{b} $wR2 = [\Sigma[w(F_o^2 - F_c^2)^2]/\Sigma[w(F_o^2)^2]]^{1/2}$. ^{c} $S = [\Sigma[w(F_c^2 - F_o^2)^2]/(N_{refins} - N_{params})]^{1/2}$.

reported,[30–32] but changes in stereochemistry often took place. Simple substitution occurs here with retention of the *trans* phosphine arrangement. To isolate the neutral [ReX_2-(PMe_3)$_2$(biimH)] compounds (**7**–**9**), a biimidazole N–H group is deprotonated by adding one equivalent of sodium methoxide to the cationic compound dissolved in methanol. The mixture changes from orange to red (from orange-brown to dark red-brown for **9**) and a solid precipitates instantly. The violet anionic species [ReX_2(PMe_3)$_2$(biim)]$^-$ are observed in CH_2Cl_2 solution when two equivalents of methoxide are added, but attempts to precipitate them (with PPh_4^+, NMe_4^+, Na^+) invariably led to mixtures containing some less soluble neutral [ReX_2(PMe_3)$_2$(biimH)].

In the mass spectra of **4**–**6**, the $(M)^+$ parent ion, unambiguously identified from isotopic distribution (^{35,37}Cl, ^{79,81}Br, ^{185,187}Re), always appears as the most intense signal. A slightly weaker signal is also found for $(M - H)^+$. The next signal corresponds to the $(M - PMe_3)^+$ fragment, as noted for the PPh_3 analogues,[19] but in the present case, its intensity relative to that of the parent ion is substantially lower. This is consistent with the Re–P bond with the better σ-donor PMe_3 ligand being stronger than with PPh_3. Very weak signals are detected for $(M - 2PMe_3)^+$ fragments.

Besides the many biimidazole absorptions, the IR spectra of all compounds give a band around 950 cm^{-1} for PMe_3. The N–H stretching region is very sensitive to the protonation state. In the deprotonated complexes **7**–**9**, the broad multicomponent N–H band is centred at ≈2500 cm^{-1}, whereas it is displaced to ≈3000 cm^{-1} for the cationic compounds **4**–**6**. The molecules in **7**–**9** are associated in pairs *via* strong complementary N–H ··· N hydrogen bonds (see crystal structures below). This results in weaker N–H bonds compared with those of the NH ··· X^- systems found in the ion pairs of **4**–**6**, and consequently to a lower vibration frequency.[33]

Even though compounds **4**–**9** are paramagnetic, their ^{1}H NMR spectra are clear. Various trends noted with the [ReX_2-(PPh_3)$_2$(biimH_2)]$^+$ complexes[19] are followed here as well. The C–H signals in **4**–**6** are both displaced upfield from their diamagnetic values (≈7 ppm). However, their displacements are 1–2 ppm less than those found for the PPh_3 analogues, where the biimidazole ligands experience the anisotropic effect of nearby phenyl rings. The H4 protons, closer to the paramagnetic centre, undergo a large upfield shift to *ca.* −2.2 ppm. The H5 signal is less displaced, but it is more sensitive to the halide present: 0.74, 1.25 and 2.33 ppm for X = Cl, Br and I, respectively. In the neutral species **7**–**9**, the corresponding resonances are displaced 4–5 ppm upfield. The absence of well-defined N–H signals and C–H signals somewhat broader than those of the PPh_3 complexes are indicative of faster exchange processes. This is consistent with the smaller size of the PMe_3 complexes, which allows the molecules to get closer together than the PPh_3 complexes.

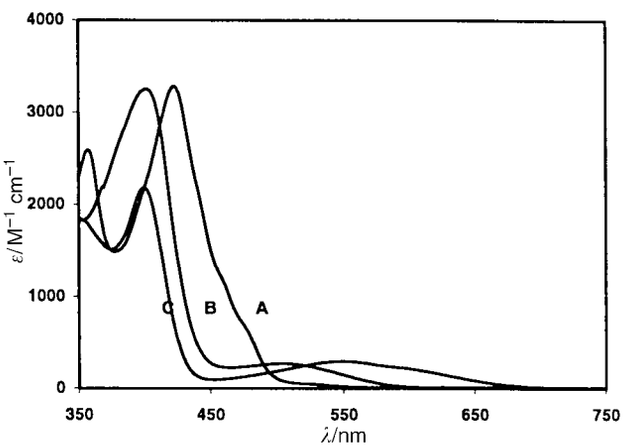

Fig. 1 UV-visible spectra of 0.0059 M solutions of [$ReCl_2$(PMe_3)$_2$(biimH_2)]$^+$ (**4**) (A), [$ReCl_2$(PMe_3)$_2$(biimH)] (**7**) (B) and [$ReCl_2$(PMe_3)$_2$(biim)]$^-$ (C) in CH_2Cl_2.

The PMe_3 signal at ≈0.8 ppm is found to be shifted to ≈1.9 ppm in $ReOCl_3(PMe_3)_2$.[32] In our cationic complexes **4**–**6**, paramagnetism displaces this signal downfield to 7.64 (Cl), 7.08 (Br) and 5.93 (I) ppm. Similar chemical shifts were observed for the methyl groups of PMe_2Ph in related complexes with bipyridine.[34] Deprotonation to form **7**–**9** shifts the PMe_3 signal upfield by ≈1 ppm.

The UV-visible spectra of **4**–**6** exhibit bands likely due to charge transfer processes, since they are too strong to correspond to d–d transitions. The spectrum of **4** is shown in Fig. 1 (curve A). The 422 nm band shifts to 441 and 493 nm as Cl is replaced by Br and I, respectively. A similar variation was noted for the related PPh_3 compounds.[19]

When the biimidazole N–H protons of [$ReCl_2$(PMe_3)$_2$-(biimH_2)]$^+$ are removed by adding one, then two, equivalents of $NaOCH_3$, the orange solution turns red, then violet, as [$ReCl_2$(PMe_3)$_2$(biimH)] and [$ReCl_2$(PMe_3)$_2$(biim)]$^-$ successively form. These two species give rise to weak bands ($\varepsilon \approx 280$ M^{-1} cm^{-1}) at 504 and 540 nm (Fig. 1), respectively, undoubtedly due to d–d transitions. For [$ReCl_2$(PMe_3)$_2$(biimH_2)]$^+$, the d–d transition probably occurs at lower wavelength, where it is

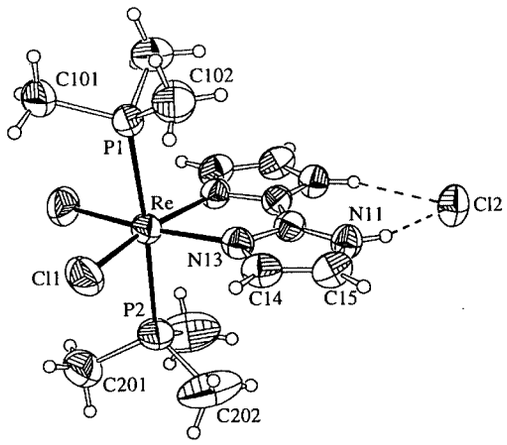

Fig. 2 ORTEP[49] drawing of $[ReCl_2(PMe_3)_2(biimH_2)]Cl$ (**4**). The molecule lies on a crystallographic mirror plane including Re, P1, P2 and Cl2. Ellipsoids correspond to 40% probability. Dashed lines represent hydrogen bonds.

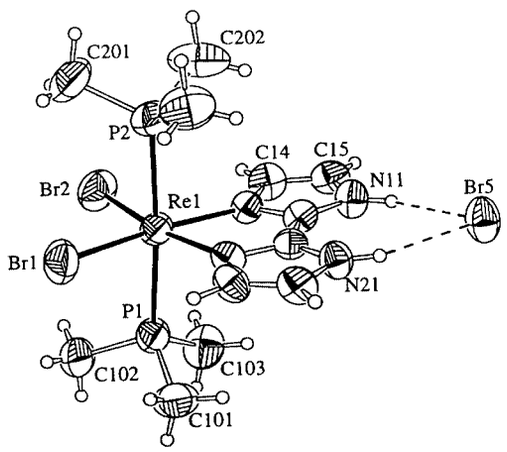

Fig. 3 ORTEP drawing of $[ReBr_2(PMe_3)_2(biimH_2)]Br$ (**5**). Ellipsoids correspond to 40% probability. Dashed lines represent hydrogen bonds.

masked by a charge-transfer band. A shoulder at ≈475 nm could have this origin.

Crystallographic studies

Crystal structures were determined for **4**, **5**, **7** and **9**. In all cases, the metal has a slightly distorted octahedral co-ordination, consisting of a chelating bidentate biimidazole unit, two mutually *trans* PMe_3 ligands and two *cis* halogens. Compounds **4** (Fig. 2) and **5** (Fig. 3) contain $[ReX_2(PMe_3)_2(biimH_2)]^+$ ions, in which biimidazole retains its two N–H protons and N–H ··· X^- hydrogen bonding with the counter-anion creates ion pairs. In **7**, biimidazole has lost one proton and the resulting neutral complex is associated in pairs *via* two complementary N–H ··· N hydrogen bonds (Fig. 4). Compound **9** is the iodo analogue of **7** and it is similarly paired *via* hydrogen bonding (Fig. 5). The lattice also includes independent Ph_3PO molecules making no particular contact with the complex. Phosphine oxide formed from displaced PPh_3, when the mixture from the reaction of $[ReI_2(PPh_3)_2(biimH_2)]I$ with PMe_3 was left to precipitate in open air.

Selected bond lengths and angles are listed in Table 2. As noted earlier for biimidazole rhenium compounds,[19,35] departure from octahedral geometry around the Re centre results mainly from the small bite angle of biimidazole (≈76°). Reduction of steric hindrance in the equatorial plane allows the halogen ligands to move away from each other and increase the X–Re–X angles to 97–100°. The P–Re–P moiety is close to linearity (≈176°), whereas the P–Re–X and P–Re–N angles remain between 86.6 and 93.3°.

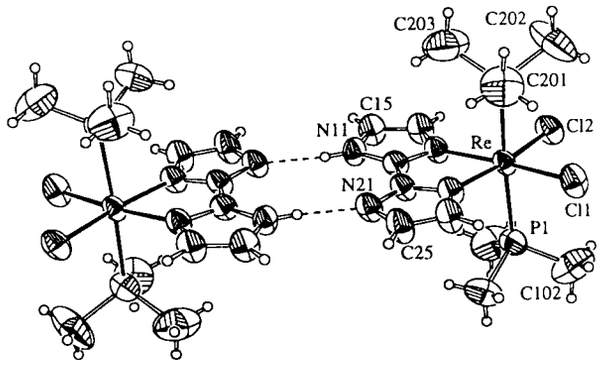

Fig. 4 ORTEP drawing of a dimeric unit of $[ReCl_2(PMe_3)_2(biimH)]$ (**7**). The two molecules are related by a crystallographic inversion centre. Ellipsoids correspond to 40% probability. Dashed lines represent hydrogen bonds.

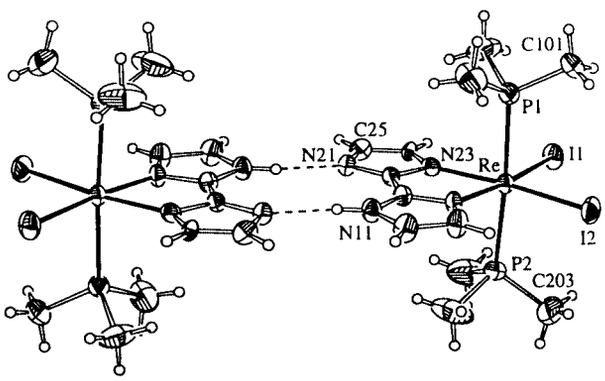

Fig. 5 ORTEP drawing of a dimeric unit of $[ReI_2(PMe_3)_2(biimH)]$ in the **9**·$OPPh_3$ compound. The two molecules are related by a crystallographic inversion centre. Ellipsoids correspond to 40% probability. Dashed lines represent hydrogen bonds. The asymmetric unit also contains a "lattice" $OPPh_3$ molecule (not shown).

The Re–N and the Re–P bond lengths in these four compounds are not significantly affected by the overall charge or the change of halide. However, the Re–Cl bonds of the cationic complex **4** (2.341(2) Å) are significantly shorter than those of the neutral analogue **7** (2.355(3), 2.378(3) Å), as one would expect, whereas the Cl–Re–Cl angle is 2.6° greater (99.7(1)° in **4** *vs.* 97.1(1)° in **7**).

The main structural difference with respect to the $[ReX_2(PPh_3)_2(biimH_2)]X$ compounds[19] is the Re–PMe_3 bonds being ≈0.04 Å shorter, in agreement with the small size and greater basicity of this phosphine.[36] Also, the Re–Cl bonds (2.341(2) Å) are significantly shorter than in the corresponding PPh_3 complex (2.381(1), 2.354(1) Å), but no similar effect is detected on the Re–Br bonds for the bromo complexes. However, in both cases, the X–Re–X angles are 2–3° smaller in the PMe_3 compounds.

Biimidazole shows the usual distortions imposed by chelate formation: the N–C2–C2′ angles inside and outside the chelate ring show large differences (≈116° and ≈133°, respectively), whereas the nitrogen lone pairs are not directed along the N–Re vector (Re–N–C angles of ≈116° inside and ≈138° outside).

Despite the fact that the halide and biimidazole ligands create very little hindrance to rotation about the Re–P bond, the methyl group on the side of the Re–X bonds adopts a staggered orientation, so that the projection of this P–C bond onto the ReX_2N_2 plane is close to the bisector of the X–Re–X angle: the (small) X–Re–P–C torsion angles vary from 28 to 47° (the bisecting position would correspond to ≈50°). For **4**, **5** and **9**, the phosphines have their P–C bonds roughly above one another, so that the ReX_2N_2 plane is an approximate mirror plane. This pseudo-mirror is not retained in **7**, since the phosphines are rotated in *opposite* directions with respect to

Table 2 Selected bond lengths (Å) and angles (°)

	4·0.8$C_4H_{10}O$·0.4CH_2Cl_2	**5**·1.1$C_4H_{10}O$ [a]	**7**	**9**·$OPPh_3$
	X = Cl	X = Br	X = Cl	X = I
Re–N(13)	2.120(6)	2.129(8)	2.097(7)	2.112(5)
Re–N(23)	—	2.125(8)	2.115(8)	2.136(6)
Re–X(1)	2.341(2)	2.500(3)	2.355(3)	2.7049(6)
Re–X(2)	—	2.493(2)	2.378(3)	2.6988(6)
Re–P(1)	2.435(3)	2.441(3)	2.434(3)	2.445(2)
Re–P(2)	2.443(3)	2.440(3)	2.421(4)	2.447(2)
N(11) ··· X(3)	3.110(6)	3.273(9)	—	—
N(21) ··· X(3)	—	3.258(9)	—	—
N(11) ··· N(21)	—	—	2.775(11)	2.758(8)
N(13)–Re–N(23)	76.1(3)	76.4(3)	75.3(3)	76.4(2)
X(1)–Re–X(2)	99.65(13)	100.01(8)	97.05(10)	97.46(2)
P(2)–Re–P(1)	175.79(9)	176.07(10)	176.45(11)	175.41(7)
N(13)–Re–X(1)	92.09(17)	168.1(2)	168.5(2)	170.76(15)
N(13)–Re–X(2)	168.20(16)	91.9(2)	94.2(2)	91.78(15)
N(23)–Re–X(1)	—	91.7(3)	93.4(2)	94.33(14)
N(23)–Re–X(2)	—	168.2(2)	169.5(2)	168.20(14)
N(13)–Re–P(1)	93.28(14)	93.3(2)	92.6(3)	90.39(16)
N(13)–Re–P(2)	90.03(14)	90.3(2)	90.9(3)	88.87(16)
N(23)–Re–P(1)	—	92.3(2)	91.2(3)	87.42(15)
N(23)–Re–P(2)	—	90.2(2)	89.9(3)	88.01(15)
X(1)–Re–P(1)	88.27(7)	87.95(11)	89.97(12)	89.41(5)
X(2)–Re–P(1)	—	88.76(10)	87.88(11)	92.31(5)
X(1)–Re–P(2)	89.02(7)	88.87(11)	86.60(13)	90.59(5)
X(2)–Re–P(2)	—	89.51(10)	91.66(11)	92.24(5)
Re–N(13)–C(12)	114.8(5)	115.7(7)	116.3(6)	116.9(4)
Re–N(13)–C(14)	138.4(5)	138.9(8)	137.3(7)	137.7(5)
Re–N(23)–C(22)	—	114.5(7)	116.8(6)	114.2(4)
Re–N(23)–C(24)	—	139.2(8)	138.4(7)	141.6(4)
N(11)–C(12)–C(22)	133.1(4)	133.9(10)	132.5(9)	132.1(6)
N(13)–C(12)–C(22)	117.0(4)	115.0(10)	116.0(8)	115.0(6)
N(21)–C(22)–C(12)	—	130.8(10)	131.1(9)	131.8(6)
N(23)–C(22)–C(12)	—	118.2(10)	115.4(9)	117.5(6)
N(11)–H(11) ··· X(3)	152.6	154.7	—	—
N(21)–H(21) ··· X(3)	—	154.3	—	—
N(11)–H(11) ··· N(21)	—	—	167.5	158.2

[a] One of the two molecules in the asymmetric unit, the other has very similar distances and angles.

Table 3 Cyclic voltammetry data for the Re(III/II) and Re(III/IV) couples [a]

	Reduction			Oxidation			
	$E_{1/2}$ [b]/mV	$I_{p,a}/I_{p,c}$	ΔE_p/mV	$E_{1/2}$ [b]/mV	$I_{p,c}/I_{p,a}$	ΔE_p/mV	ΔE_{ox-red} [e]/mV
1	−841	1	74	718	0.86	72	1559
2	−722	0.75	72	794 [c]	0.85	118 [c]	1516
3	−606	0.48	57	806	≈1 [d]	61	1412
4	−1032	0.36	65	581	0.89	58	1613
5	−914	0.40	69	670	0.94	78	1584
6	−757	0.50	66	670	≈1 [d]	70	1427

[a] In CH_2Cl_2 (0.1 M NBu_4PF_6), scan rate = 100 mV s^{-1}. [b] $E_{1/2} = (E_{p,a} + E_{p,c})/2$. [c] Because of Br^- oxidation at the same potential, the peak is much broader and the maximum is slightly displaced to the anodic potentials, causing ΔE_p to be higher than the effective value. [d] Estimated value. The anodic current could not be measured precisely, since the second oxidation of iodide takes place just before that of Re(III). [e] $\Delta E_{ox-red} = E_{1/2(ox)} - E_{1/2(red)}$.

the bisecting position: this leads to a conformation similar to that of the PPh_3 analogues, where an approximate C_2 axis lies in the ReX_2N_2 plane, bisecting the X–Re–X and N–Re–N angles.

The N–H groups of biimidazole generally find partners in the crystals to form strong hydrogen bonds. This is the case for those of the cationic compounds **4** and **5**, where the X^- counter-ions are hydrogen-bonded to both N–H groups. In **4** (Fig. 2), N ··· Cl distances (3.110(6) Å) are on the short side of the accepted range (2.91–3.53 Å)[37] and the N–H ··· Cl angles (153°) are close to linearity. This is comparable with the N–H ··· Cl units in the PPh_3 complex[19] and in [{ORe(biimH_2)$_2$}$_2$O]Cl_4.[38] For **5** (Fig. 3), the N ··· Br^- separations (≈3.26 Å) are definitely lower than the typical value of 3.37 Å,[39] whereas the N–H ··· Br^- angles are ≈154°.

The neutral [ReX_2(PMe_3)$_2$(biimH)] compounds **7** (Fig. 4) and **9** (Fig. 5) consist of dimeric units related by a crystallographic inversion centre and connected *via* two complementary N–H ··· N hydrogen bonds. The N ··· N separations (≈2.76 Å) are below the lower limit of the range (2.88–3.38 Å) proposed for such hydrogen bonds.[37] In fact, they are even shorter than those found in imidazole[40] and biimidazole[41] crystals. Similar strong hydrogen bonds have been reported for a copper complex containing monodeprotonated biimidazole[10] and for a five-biimidazole unit in [(biimH_2)$_3$(biimH_3^+)$_2$](I$^-$)$_2$.[42]

Acidity of the N–H groups

In our previous paper, competition with carboxylic acids and phenols was used to estimate the acidities of these protons in

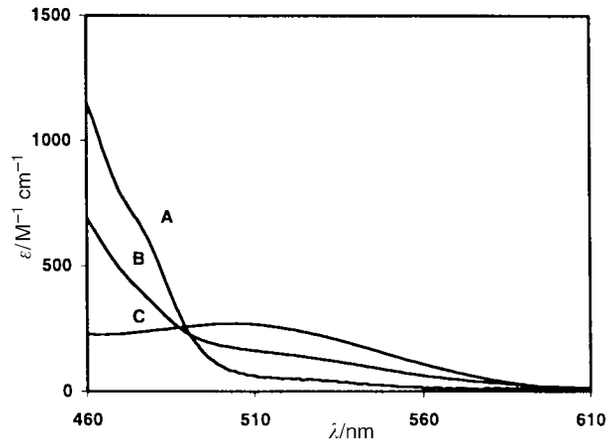

Fig. 6 Visible spectra of 0.0059 M solutions of $[ReCl_2(PMe_3)_2(biimH_2)]^+$ (**4**) (A), $[ReCl_2(PMe_3)_2(biimH)]$ (**7**) (C) and a 1 : 1 $[ReCl_2(PMe_3)_2(biimH)]$: HCOOH mixture (B) in CH_2Cl_2.

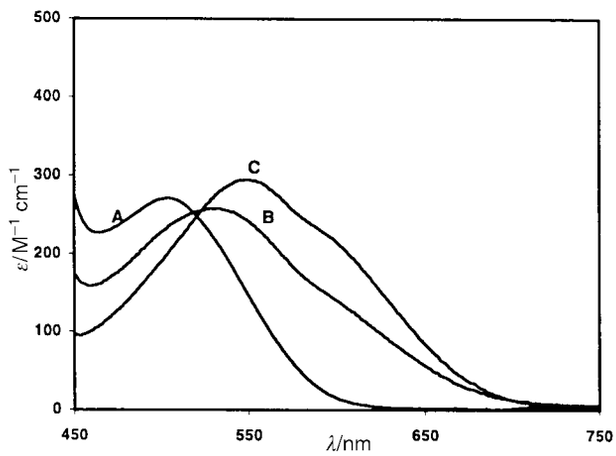

Fig. 7 Visible spectra of 0.0059 M solutions of $[ReCl_2(PMe_3)_2(biimH)]$ (**7**) (A), $[ReCl_2(PMe_3)_2(biim)]^-$ (C) and a 1 : 1 $[ReCl_2(PMe_3)_2(biim)]^-$: 3-chlorophenol mixture (B) in CH_2Cl_2.

$[ReCl_2(PPh_3)_2(biimH_2)]^+$.[19] This method is applied here to the PMe_3 compound **4**.

The first acidity is probed by deprotonating one N–H group with 1 equivalent of sodium methoxide (eqn. (1)) and then adding 1 equivalent of various carboxylic acids. Reprotonation of $[ReCl_2(PMe_3)_2(biimH)]$ (eqn. (2)) occurs when the carboxylic

$$[ReCl_2(PMe_3)_2(biimH_2)]^+ + CH_3O^- \longrightarrow [ReCl_2(PMe_3)_2(biimH)] + CH_3OH \quad (1)$$

$$[ReCl_2(PMe_3)_2(biimH)] + RCO_2H \longrightarrow [ReCl_2(PMe_3)_2(biimH_2)]^+ + RCO_2^- \quad (2)$$

acid is stronger than the N–H group of $[ReCl_2(PMe_3)_2(biimH_2)]^+$. The process can be followed visually from colour change between $[ReCl_2(PMe_3)_2(biimH_2)]^+$ (orange) and $[ReCl_2(PMe_3)_2(biimH)]$ (red). Upon addition of benzoic acid (pK_a(aq) = 4.19), the solution retains the red colour of the neutral species $[ReCl_2(PMe_3)_2(biimH)]$, whereas reprotonation to orange $[ReCl_2(PMe_3)_2(biimH_2)]^+$ takes place with chloroacetic acid (pK_a(aq) 2.85) and stronger acids. Fig. 6 shows the visible spectral region for the two forms and for a 1 : 1 mixture with formic acid. The intermediate position of the latter solution (curve B) indicates that reprotonation is roughly half-way and that the first N–H group has an acidity comparable with that of formic acid (pK_a(aq) = 3.75).[43]

To evaluate the second acidity, both N–H groups are deprotonated first with 2 equivalents of sodium methoxide (eqn. (3)) and 1 equivalent of various phenols is added. The colour

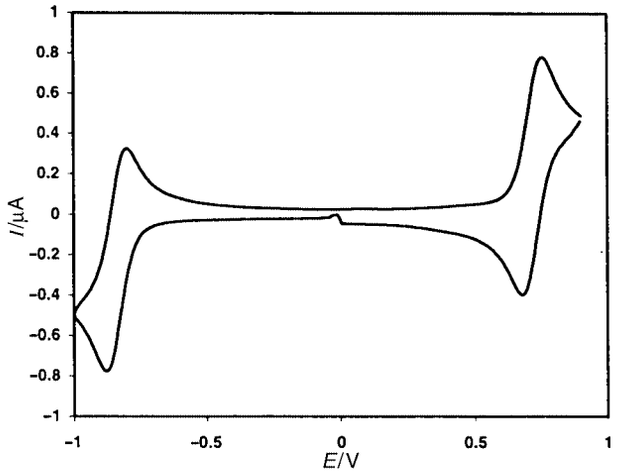

Fig. 8 Cyclic voltammogram of a 1.4×10^{-3} M solution of **1** in CH_2Cl_2 containing 0.1 M NBu_4PF_6, scan rate = 100 mV s^{-1}.

changes from violet to red when $[ReCl_2(PMe_3)_2(biim)]^-$ reprotonates to $[ReCl_2(PMe_3)_2(biimH)]$ (eqn. (4)). Curve B in Fig. 7 lies approximately half-way between those of these two forms, indicating that this N–H group has an acidity similar to that of 3-chlorophenol (pK_a(aq) = 8.85).[43]

$$[ReCl_2(PMe_3)_2(biimH_2)]^+ + 2\,CH_3O^- \longrightarrow [ReCl_2(PMe_3)_2(biim)]^- + 2\,CH_3OH \quad (3)$$

$$[ReCl_2(PMe_3)_2(biim)]^- + ArOH \longrightarrow [ReCl_2(PMe_3)_2(biimH)] + ArO^- \quad (4)$$

Under the same conditions, the acidities of $[ReCl_2(PPh_3)_2(biimH_2)]^+$ (**1**) were found to correspond to acetic acid (pK_a(aq) ≈ 4.8) and phenol (pK_a(aq) ≈ 9.8), respectively. This result is puzzling, since considerations generally applicable to acid–base processes in the gas phase or in protic solvents would lead us to predict that replacing PPh_3 by the better donor PMe_3 should make the N–H groups less acidic. However, the situation is more complicated in the aprotic CH_2Cl_2 solvent, where the species are extensively associated *via* ion pairing and hydrogen bonding. Detailed studies are needed to fully understand these associations.

Electrochemistry

The electrochemical behaviour of the present $[ReX_2(PMe_3)_2(biimH_2)]X$ compounds (**4**–**6**) and the corresponding PPh_3 complexes (**1**–**3**)[19] was investigated. The typical voltammogram shown in Fig. 8 corresponds to $[ReCl_2(PPh_3)_2(biimH_2)]Cl$ (**1**). It was established, by comparison with the Fc/Fc^+ couple, that the processes discussed here are all monoelectronic. The voltammogram exhibits one reversible oxidation process. For **2**, **3**, **5** and **6**, metal oxidation is accompanied by oxidation of the Br^- or I^- counter-ion taking place around the same potential or below. Reversibility is observed in all cases, indicating that no interactions take place with the oxidised halide. On the cathodic side, a single, generally irreversible, reduction process takes place. For both oxidation and reduction, the forward peak currents are linearly correlated with the square root of the potential scan speed, as expected for a diffusion process.

In cyclic voltammetry, all oxidation processes are reversible: the $I_{p,c}/I_{p,a}$ ratios are close to unity and the ΔE_p (= $E_{p,a} - E_{p,c}$) values range from 58 to 78 mV (Table 3), which is reasonably close to the expected 59 mV value. The oxidation potentials listed in Table 3 are generally higher than those reported for various Re(III) chloro complexes containing phosphine and/or nitrogen ligands.[34,44–46] To our knowledge, no data are available in the literature for bromo- or iodo-rhenium(III) monomers. The chloro compounds **1** and **4** ($E_{1/2}$ = 718 and 581 mV, respectively) oxidise more readily than the $[ReCl_2(PMe_2Ph)_2(bipy)]^+$

Table 4 Oxidation potential of X^- (mV)[a]

	NBu_4^+	**1**, **2**, **3**	**4**, **5**, **6**
Cl^-	1126	1475	1475
Br^-	753	850	887
I^-	284	352	335

[a] Determined by CV with 0.5 mm working electrode. Same conditions as in Table 3.

species studied by Caspar *et al.* ($E_{1/2}$ = 880 mV).[34] Since the basicity of PMe_2Ph is intermediate between those of PPh_3 and PMe_3,[36] our low oxidation potentials should be ascribed to the greater σ-donor ability of biimidazole as compared with bipyridine, making the metal centre more electron-rich.[18]

On the cathodic side, the $I_{p,a}/I_{p,c}$ ratios are much smaller than 1 for the three $[ReX_2(PMe_3)_2(biimH_2)]X$ compounds (**4**–**6**) and for $[ReI_2(PPh_3)_2(biimH_2)]I$ (**3**) and show that their reduction is irreversible (even at 100 V s^{-1}), despite the small ΔE_p values (57–69 mV). Low stability of the reduced Re(II) species is not surprising, since the Re(III) complexes are electron-rich. However, the presence of the weaker electron-donor PPh_3 ligand improves reversibility: reduction occurs reversibly for the chloro compound **1** at all sweep rates, whereas for **2**, reversibility is retained at sweep rates above 400 mV s^{-1}. This marked variation as X is changed suggests that the Re–X bond in the Re(II) species is broken first and that the halogen leaving ability is in the order $I^- > Br^- > Cl^-$. The reduction processes of **1**–**6** are observed over a wide potential range (from −1032 to −606 mV). Thus, these complexes are easier to reduce than the previously reported neutral species.[34,44–46] As expected, the greater basicity of biimidazole makes compounds **1** and **4** more difficult to reduce than the analogous $[ReCl_2(PMe_2Ph)_2(bipy)]^+$ ($E_{1/2}$ = −390 mV).

Substitution of PPh_3 by PMe_3 decreases the Re(III)/Re(IV) oxidation potentials by ≈130 mV, which is fairly close to the variation (102 mV) anticipated from the calculated potentials for these complexes using Lever's constants.[47] The latter model also predicts that the chloro and iodo complexes of a given phosphine should have the same oxidation potential, whereas oxidation of the bromo analogue should occur 34 mV higher. This pattern is not followed here, since the bromo and iodo compounds have roughly equal potentials, ≈85 mV above that of the chloro complex. Association with the halide counter-ion, whose strength increases in the series I < Br < Cl, likely affects the potential significantly and may contribute to modifying the expected order. As to the reduction process, the potentials exhibit similar variations, but with a greater amplitude. Thus, replacing PPh_3 by PMe_3 shifts the Re(III)/Re(II) reduction potentials by 150–190 mV. Greater variations are noted here as a function of the halogen: when Cl is changed to Br or I, the potential is shifted by ≈120 and ≈250 mV, respectively. For a related Re(III) bipyridine complex, Meyer and co-workers[34] found that the changes produced by phosphine replacement are smaller for the reduction than the oxidation. This could be related to the bipyridine ligand being a better π acceptor than $biimH_2$, which could more efficiently absorb charge variations on the electron-rich metal centre.

Overall, the presence of PMe_3 tends to stabilise the rhenium(III) form, since ΔE_{ox-red} is larger by ≈60 mV when analogous compounds (bromo or chloro) are compared (Table 3). Increasing the σ-donor ability of the halide has a similar effect.

In previous studies on $[ReX_2(PPh_3)_2(biimH_2)]X$ compounds, ion pairing in low-polarity solvents was proposed on the basis of high solubility in these solvents, N–H ··· X^- hydrogen bonding in the solid state and, in the case of the chloro compound, evidence that hydrogen bonding in solution is strong enough to affect the ^{1}H NMR spectra.[19] Electrochemical data provide further support that ion pairing does take place in CH_2Cl_2 solution, even for the heavier halides. Oxidation potentials of X^- are listed in Table 4 for the complexes and the Bu_4N^+ salts. For Cl^-, a huge difference of 349 mV is noted between Bu_4N^+ and **1** or **4**. Thus, electron density of the Cl^- counter-ion is considerably decreased in the complexes, making it much more difficult to oxidise. This provides extra experimental evidence that Cl^- remains tightly bound to co-ordinated $biimH_2$ in solution. Smaller, but very significant, differences are found for Br^- (≈120 mV) and I^- (≈60 mV) as well. Therefore, even though these heavier halides are not considered to form strong hydrogen bonds,[39,48] some association is clearly found to take place.

Concluding remarks

Stable Re(III) cationic monomers $[ReX_2(PMe_3)_2(biimH_2)]X$ are obtained smoothly and with retention of stereochemistry by reacting the PPh_3 analogues with excess PMe_3. These complexes are readily deprotonated and the neutral $[ReX_2(PMe_3)_2(biimH)]$ compounds can be isolated as hydrogen-bonded dimeric species. Both the cationic and the neutral forms exhibit good stability. Electrochemical data provide further evidence that hydrogen bonding between co-ordinated biimidazole and halide counter-ions is retained, thereby supporting the conclusions drawn earlier from ^{1}H NMR spectra.[19] The relatively high acidity of the N–H protons renders these complexes easy to deprotonate and makes them promising candidates to prepare bis-bidentate biimidazolate-bridged dinuclear materials.

Acknowledgements

The authors wish to thank Dr F. D. Rochon for collecting the X-ray data on compound **9**, F. Bélanger-Gariépy and Dr M. Simard for assistance with the other crystal structures, and A. Mari for the magnetic measurements. The financial support of Natural Sciences and Engineering Research Council of Canada is gratefully acknowledged.

References

1 C. Savoie, C. Reber, S. Bélanger and A. L. Beauchamp, *Inorg. Chem.*, 1995, **34**, 3851.
2 C. Savoie and C. Reber, *Coord. Chem. Rev.*, 1998, **171**, 387.
3 C. Savoie and C. Reber, *J. Am. Chem. Soc.*, 2000, **122**, 844.
4 H. H. Thorp, C. V. Kumar, N. J. Turro and H. B. Gray, *J. Am. Chem. Soc.*, 1989, **111**, 4364.
5 H. H. Thorp, J. V. Houten and H. B. Gray, *Inorg. Chem.*, 1989, **28**, 889.
6 J. R. Winkler and H. B. Gray, *Inorg. Chem.*, 1985, **24**, 346.
7 J. R. Winkler and H. B. Gray, *J. Am. Chem. Soc.*, 1983, **105**, 1373.
8 M. Takodoro and K. Nakasuji, *Coord. Chem. Rev.*, 2000, **198**, 205.
9 M. Takodoro, K. Isobe, H. Uekusa, Y. Ohasi, J. Toyoda, K. Tashiro and K. Nakasuji, *Angew. Chem., Int. Ed.*, 1999, **38**, 95.
10 M. Takodoro, J. Toyoda, K. Isobe, T. Itoh, A. Miyasaki, T. Enoki and K. Nakasuji, *Chem. Lett.*, 1995, 613.
11 S. Rau, T. Büttner, C. Temme, M. Ruben, H. Görls, D. Walther, M. Duati, S. Fanni and J. G. Vos, *Inorg. Chem.*, 2000, **39**, 1621.
12 M. Haga, T. Matsumura-Inoue and S. Yamabe, *Inorg. Chem.*, 1987, **26**, 4148.
13 P. Majumdar, S.-M. Peng and S. Goswani, *J. Chem. Soc., Dalton Trans.*, 1998, 1569.
14 A. P. de Silva, H. Q. N. Gunaratne, T. Gunnlaugsson, A. J. M. Huxley, C. P. McCoy, J. T. Rademacher and T. E. Rice, *Chem. Rev.*, 1997, **97**, 1515.
15 M. D. Ward, *Chem. Soc. Rev.*, 1995, **24**, 121.
16 M. P. Garcia, A. M. Lopez, M. A. Esteruelas, F. J. Lahoz and L. A. Oro, *J. Chem. Soc., Chem. Commun.*, 1988, 793.
17 M. A. Esteruelas, M. P. Garcia, A. M. Lopez and L. A. Oro, *Organometallics*, 1991, **10**, 127.
18 D. P. Rillema, R. Sahai, P. Matthews, A. K. Edwards, R. J. Shaver and L. Morgan, *Inorg. Chem.*, 1990, **29**, 167.
19 S. Fortin and A. L. Beauchamp, *Inorg. Chem.*, 2001, **40**, 105.
20 G. Foëx, *Tables de Constantes et Données Numériques–Diamagnétisme et Paramagnétisme*, Masson, Paris, 1957.
21 Enraf-Nonius, CAD-4 Software, Version 5.0, Enraf-Nonius, Delft, The Netherlands, 1989.

22 XSCANS, Bruker Analytical X-Ray Systems, Madison, WI, USA, 1995.
23 E. J. Gabe, Y. LePage, J. P. Charland, F. L. Lee and P. S. White, *J. Appl. Crystallogr.*, 1989, **22**, 384.
24 F. R. Ahmed, S. R. Hall, M. E. Pippy and C. P. Huber, NRC Crystallographic Computer Programs for the IBM/360, Accession Nos. 133–147 in *J. Appl. Crystallogr.*, 1973, **6**, 309.
25 G. M. Sheldrick, SHELXS-86, Program for the Solution of Crystal Structures, University of Göttingen, Göttingen, Germany, 1990.
26 G. M. Sheldrick, SHELXL-93, Program for the Refinement of Crystal Structures, University of Göttingen, Göttingen, Germany, 1993.
27 G. M. Sheldrick, SHELXTL, Bruker AXS Inc., Madison, WI, USA, 1995.
28 A. L. Spek, PLATON, Molecular Geometry Program (July 1995 version), University of Utrecht, Utrecht, The Netherlands, 1995.
29 Autolab GPES, Version 4.5, EcoChemie B.V., Utrecht, The Netherlands, 1997.
30 J. Chatt, J. D. Garforth, N. P. Johnson and G. A. Rowe, *J. Chem. Soc.*, 1964, 601.
31 G. Rouschias, *Chem. Rev.*, 1974, **74**, 531.
32 A. L. Ondracek, P. E. Fanwick and R. A. Walton, *Inorg. Chim. Acta*, 1998, **267**, 123.
33 M. D. Joesten, *J. Chem. Educ.*, 1982, **59**, 362.
34 J. V. Caspar, B. P. Sullivan and T. J. Meyer, *Inorg. Chem.*, 1984, **23**, 2104.
35 S. Fortin and A. L. Beauchamp, *Inorg. Chem.*, 2000, **39**, 4886.
36 M. M. Rahman, H. Y. Liu, A. Prock and W. P. Giering, *Organometallics*, 1987, **6**, 650.
37 G. H. Stout and L. H. Jensen, *X-Ray Structure Determination, A Practical Guide*, The Macmillan Company, London, 1968.
38 S. Bélanger and A. L. Beauchamp, *Acta Crystallogr., Sect. C*, 1999, **55**, 517.
39 G. C. Pimentel and A. L. McClellan, *Annu. Rev. Phys. Chem.*, 1971, **22**, 347.
40 S. Martinez-Carrera, *Acta Crystallogr.*, 1966, **20**, 783.
41 D. T. Cromer, R. R. Ryan and C. B. Storm, *Acta Crystallogr., Sect. C*, 1987, **43**, 1435.
42 T. Akutagawa, G. Saito, M. Kusunoki and K. I. Sakaguchi, *Bull. Chem. Soc. Jpn.*, 1996, **69**, 2487.
43 *CRC Handbook of Chemistry and Physics, 75th edition, Special Students Edition*, ed. D. R. Lide, Chemical Rubber Company Press, Boca Raton, FL, 1997.
44 S. Bhattacharyya, S. Banerjee, B. K. Dirghangi, M. Menon and A. Chakravorty, *J. Chem. Soc., Dalton Trans.*, 1999, 155.
45 J. R. Dilworth, P. Jobanputra, J. R. Miller, S. J. Parrott, Q. Chen and J. Zubieta, *Polyhedron*, 1993, **12**, 513.
46 J. R. Kirchhoff, W. R. Heineman and E. Deutsch, *Inorg. Chem.*, 1987, **26**, 3108.
47 A. B. P. Lever, *Inorg. Chem.*, 1990, **29**, 1271.
48 W. C. Hamilton and J. A. Ibers, *The Hydrogen Bonding in Solids*, Benjamin, New York, 1968.
49 C. K. Johnson, ORTEP, Report ORNL-5138, Oak Ridge National Laboratory, Oak Ridge, TN, 1976.